

A spectral method in space and time to solve the advection-diffusion and wave equations in a bounded domain.

Pétri, Jérôme

*Observatoire Astronomique de Strasbourg, Université de Strasbourg, CNRS, UMR 7550,
11 rue de l'Université, 67000 Strasbourg, France.*

Abstract

The advection-diffusion and wave equations are the fundamental equations governing any physical law and therefore arise in many areas of physics and astrophysics. For complex problems and geometries, only numerical simulations can give insight into quantitative and accurate behavior of the sought solutions. The standard numerical algorithm to solve partial differential equations is to split the space and time discretisation separately into different uncorrelated methods. Time is usually advanced by explicit schemes, or, for too restrictive time steps, by implicit or semi-implicit algorithms. This separate time and space slicing is artificial and sometimes unpractical. Indeed, treating space and time directions symmetrically and simultaneously without splitting is highly recommended in some problems like diffusion.

It is the purpose of this work to present a simple numerical algorithm to solve the standard linear scalar advection-diffusion and wave equations using a fully spectral method in a two-dimensional Cartesian (x, t) bounded space-time domain. Generalization in three-dimensions (x, y, t) (two space dimensions) is straightforward and shown for the pure diffusion problem. The basic idea is to expand the unknown function in Chebyshev polynomials for the spatial variables (x, y) as well as for the time variable t . We show typical examples and demonstrate the spectral accuracy of the method. Nevertheless, we emphasize that the method requires to invert a large matrix that can be very time and memory consuming, especially for high resolution and/or higher dimensional problems. This occurs already for modest resolutions in two-dimensions like a grid of 129×129 points in (x, t) . It becomes even more severe for three dimensions, we were unable to deal with resolution higher

than $33 \times 33 \times 33$. The next step would be to supersede the straightforward direct inversion matrix operation by a more efficient and less memory demanding algorithm to solve large linear systems. This is unavoidable if one wants to study higher spatial dimensional setups. The aim of this study is to demonstrate the feasibility of such codes. Moreover, the great advantage of fully spectral methods resides in their high-accuracy for a relatively small number of grid points (for sufficiently smooth solutions) compared to standard time-stepping techniques.

Key words: Spectral methods, Chebyshev polynomials, Wave, Advection, Relativity

1. Introduction

Any physical law is represented in an abstract space called space-time. Physically meaningful quantities evolve in space and time with prescribed spatial and temporal relations. Mathematically, this is translated into a set of partial differential equations (PDEs) with appropriate initial and boundary conditions to obtain a well-posed problem. They describe the fundamental behavior of any physical system by local interactions. Analytical solutions are very difficult to find and are only available for a very restricted number of PDEs and configurations. Therefore, looking for numerical solutions to these PDEs is an important task in order to make any prediction or fitting observations and experiments.

Several techniques allow to study the behavior of physical systems by looking for numerical solutions of the corresponding PDEs. Finite difference is the most common technique and most straightforward one, sampling space and time on a finite grid. For shocks in hydrodynamical or MHD flows, finite volume schemes are preferred in order to conserve, within machine accuracy, physical quantities such as total energy and momentum if required.

Spectral or pseudo-spectral methods expand the unknown functions on a well chosen basis of polynomials or other special functions, depending on the geometry and on the boundary conditions.

Particle in cell simulations are common in plasma physics where wave/particle interactions can produce some significant effects not seen in an MHD or multi-fluid picture [1, 9]. They combine a set of charged particles to the ambient electromagnetic field via Maxwell equations.

For spatially multidimensional problems, one has the freedom to choose the most convenient method for each direction independently. For instance in cylindrical geometry, Fourier spectral method in the azimuthal direction, finite volume in the radial direction and finite difference in time.

Splitting the PDE into a space and a time direction is arbitrary. From the theory of general relativity, we know that covariance implies to treat space and time on the same level. Such approach can reveal very fruitful to investigate relativistic stars in general relativity.

An extensive literature on spectral method with Fourier, Chebyshev and Legendre transforms can be found in [2] with applications to different geometries. Specific examples for fluid dynamics are reported in [4, 5] for single and multi-domain complex flows. It is well known that discontinuities, such as shocks appearing in fluid mechanics, give rise to the Gibbs phenomenon, degrading the convergence properties of any spectral method. This is usually circumvented by introducing some filtering or smoothing, applying artificial viscosity for instance. This is an ongoing active research field [6].

Spectral methods in time have been used to solve the Korteweg de Vries and Burger equations with spatial periodic solutions, expanded in Fourier series, [10]. Applications to relativistic situations has been undertaken by Hennig and Ansorg [8]. Here we follow the same method, namely, expansion of the unknown function in terms of Chebyshev polynomial with respect to space and time coordinate and reformulation of the initial-boundary value problem in terms of an algebraic system for the Chebyshev coefficients or equivalently, for the function values at the collocation points. They solved the wave equation in Minkowski space-time for the spherically symmetric geometry. In order to avoid artificial boundary condition at a finite distance, they used a compactification method. Contrary to their work, we restrict to spatially compact domain and linear equations (solved by direct method compared to their Newton-Raphson method allowing to treat also non-linear problems) of first and second order. A review on (pseudo-)spectral methods emphasizing astrophysical applications can be found in [7].

In this paper, we design a fully implicit spectral method to solve PDEs in one space dimension with fixed and outgoing wave boundary conditions, using a Cartesian coordinate system. Two spatial dimensions are also briefly discussed. Because of the lack of periodicity in the computational bounded domain, Chebyshev polynomial expansion is highly recommended in both space and time directions. Useful properties about Chebyshev polynomials are reminded in section 2. Next, in section 3 we determine the linear ad-

vection operator to solve the full advection equation with general boundary conditions. The same procedure is then applied in section 4 for the linear wave operator in order to solve the wave equation with outgoing or fixed boundary conditions. Section 5 depicts the diffusion equation in two spatial dimensions. Results and tests for these simple examples are shown in section 6 before concluding in section 7.

2. A reminder on Chebyshev polynomials

We start by recalling some important features of Chebyshev polynomials as well as some useful properties about their derivatives.

In the most general compact computational domain, the space-time interval is $(x, t) \in [a, b] \times [t_1, t_2]$. Without loss of generality, it is always possible to introduce new independent variables (ζ, τ) such that the scaling is recast into the range $(\zeta, \tau) \in [-1, 1] \times [-1, 1]$ by a linear mapping. For completeness, this mapping looks like

$$x = \frac{b-a}{2}\zeta + \frac{b+a}{2} \quad (1)$$

where the variable ζ lies in the window $[-1, 1]$. The same linear transformation would apply to the time coordinate t replaced by τ or any other spatially bounded variable. We restrict our discussion to this normalized domain.

2.1. Definition and properties

Chebyshev polynomials, denoted by $T_k(x)$, are defined in the interval $x \in [-1, 1]$ such that

$$T_k(x) = \cos(k \arccos(x)) \quad (2)$$

where k is a positive integer. Their boundary values as well as those of their first and second derivatives are easily found to be

$$T_k(\pm 1) = (\pm 1)^k \quad (3)$$

$$T'_k(\pm 1) = (\pm 1)^{k+1} k^2 \quad (4)$$

$$T''_k(\pm 1) = (\pm 1)^k k^2 \frac{k^2 - 1}{3} \quad (5)$$

These results are useful to impose special boundary conditions of Dirichlet, Neumann or Robin type, as we will see later.

2.2. Interpolation function

Any well behaved function $f(x)$, let us say continuous as well as several of its derivatives, defined on the interval $[-1, 1]$, is expanded in a series of Chebyshev polynomials. The interpolation of f containing N terms is denoted by f_N and written as

$$f_N(x) = \sum_{k=0}^{N-1} f_k T_k(x) \quad (6)$$

f_k are the coefficients of the expansion. Chebyshev polynomials are closely related to the trigonometric cosines functions as seen from their definition Eq. (2). The series Eq. (6) can therefore be computed by a Fourier cosines transform, employing a Fast Fourier Transform (FFT) algorithm. Because of the relation with the FFT algorithm, the first term f_0 appears usually with a factor $1/2$ [11]. Here we suppress this normalization factor of the constant coefficient for later convenience when dealing with the different linear operators and matrices. We emphasize that for computational domains that are not normalized, linear transformations such that those of Eq.(1) can be useful. The Chebyshev series expansion is computed most efficiently and accurately with help on FFTs. The function f is discretised on a grid corresponding to the Gauss-Lobatto collocation points defined by

$$\xi_i = \cos\left(\frac{i \pi}{N-1}\right) \quad (7)$$

with $i \in [0..N-1]$. This links the coefficients in the Chebyshev space to the real physical space. In the remainder of this paper, we will assume that $(x, t) \in [-1, 1]^2$ (therefore renaming (ζ, τ) into (x, t)).

For PDEs, partial differentiation of the unknown quantities at any order with respect to one coordinate, space or time, is required. We therefore look for the relation between the coefficient of the derivative of any order to the coefficient of the interpolant function itself. This is compulsory in order to solve the discretised problem and is explained in the next paragraph.

2.3. Derivative operator

Differentiation of f can be interpreted as an algebraic multiplication in the coefficient space. Indeed, let any function $f(x)$ possess an approximate

series expansion with Chebyshev coefficients f_k given by Eq. (6). Those of its first derivative f' are given by a simple matrix multiplication

$$f'_k = \sum_{i=0}^{N-1} \mathcal{D}_{ki} f_i \quad (8)$$

with $k \in [0..N-1]$. The matrix representation of the derivative operator in the Chebyshev coefficient space reads

$$\mathcal{D}_{ik} = \begin{pmatrix} 0 & 1 & 0 & 3 & 0 & \dots & k & \dots & N-1 \\ 0 & 0 & 4 & 0 & 8 & & 0 & \dots & 0 \\ 0 & 0 & 0 & 6 & 0 & & 2k & \dots & 2(N-1) \\ 0 & 0 & 0 & 0 & 8 & & 0 & \dots & 0 \\ \vdots & 0 & 0 & 0 & 0 & \ddots & \vdots & & \vdots \\ \vdots & 0 & 0 & 0 & 0 & \ddots & 2k & & 0 \\ \vdots & & & & & \dots & 0 & & 2(N-1) \\ 0 & & & & & \dots & & & 0 \end{pmatrix} \quad (9)$$

It is an upper triangular matrix with its diagonal terms equal to zero.

The same procedure can be repeated for higher order derivatives of order n denoted by $f^{(n)}$. We need only to take the corresponding power of the matrix \mathcal{D}_{ik} such that the coefficient of $f^{(n)}$ are

$$f_k^{(n)} = \sum_{i=0}^{N-1} (\mathcal{D}_{ki})^n f_i \quad (10)$$

We summarize the results by writing the expansion of the n -th derivative of the interpolant as

$$f_N^{(n)}(x) = \sum_{i=0}^{N-1} \sum_{k=0}^{N-1} (\mathcal{D}_{ki})^n f_i T_k(x) \quad (11)$$

2.4. Product

For linear differential operators such as the Laplacian or for an arbitrary linear combination of partial derivatives, it is helpful to find a matrix expression of that operator in the coefficient space.

In order to work out this operator explicitly, we need to relate the coefficients of a product of two functions to those of these two functions. Let

us be two functions f and g defined in $[-1, 1]$. Given their respective expansion coefficients f_k and g_k for their interpolant f_N and g_N , we look for the expression of the coefficient of their product $f_N g_N$. These are found by introducing another “matrix” possessing three indices and denoted by \mathcal{P}_{ikl} , with $(i, k, l) \in [0..N-1]^3$, such that

$$(f_N g_N)_i = \sum_{k=0}^{N-1} \sum_{l=0}^{N-1} \mathcal{P}_{ikl} f_k g_l \quad (12)$$

For concreteness, the first elements of this matrix are reported explicitly in the following lines. The first “sub-matrix” is diagonal and reads

$$\mathcal{P}_{0kl} = \begin{pmatrix} 1 & 0 & \dots & & 0 \\ 0 & 1/2 & \ddots & & \vdots \\ \vdots & \ddots & 1/2 & \ddots & \vdots \\ \vdots & & \ddots & \ddots & 0 \\ 0 & \dots & \dots & 0 & 1/2 \end{pmatrix} \quad (13)$$

The second submatrix has a vanishing diagonal such that

$$\mathcal{P}_{1kl} = \begin{pmatrix} 0 & 1 & 0 & \dots & 0 \\ 1 & 0 & 1/2 & \ddots & \vdots \\ 0 & 1/2 & \ddots & \ddots & 0 \\ \vdots & \ddots & \ddots & \ddots & 1/2 \\ 0 & \dots & 0 & 1/2 & 0 \end{pmatrix} \quad (14)$$

and, finally, the third submatrix is

$$\mathcal{P}_{2kl} = \begin{pmatrix} 0 & 0 & 1 & 0 & \dots & 0 \\ 0 & 1/2 & 0 & 1/2 & \ddots & \vdots \\ 1 & 0 & 0 & \ddots & \ddots & 0 \\ 0 & 1/2 & \ddots & \ddots & \ddots & 1/2 \\ \vdots & \ddots & \ddots & \ddots & 0 & 0 \\ 0 & \dots & 0 & 1/2 & 0 & 0 \end{pmatrix} \quad (15)$$

The remaining submatrices for $i > 2$ can be deduced easily. Note that all these submatrices are symmetric with respect to the last two indices k and l owing to the symmetry of the product of two functions, i.e. $f_N g_N = g_N f_N$.

With the derivatives and the multiplication defined as matrices given above, any linear differential operator in space and time can be written in any number of spatial dimensions. For instance, the operators

$$\frac{1}{x} \frac{\partial}{\partial x} \tag{16}$$

and

$$\frac{1}{x^2} \frac{\partial^2}{\partial x^2} \tag{17}$$

are encountered when expressing the Laplacian in cylindrical and spherical geometry. This is very useful for deriving the matrix operator according to such linear differential operator.

In the following sections, two straightforward applications are shown for the advection and wave equations. They serve as a starting point to check the numerical algorithm and look for the convergence properties before shifting to more advanced schemes dealing with several geometries and several unknown functions. However, these complications are left for future work. Nevertheless, the two space dimensions set up is discussed in the constant coefficient diffusion problem.

3. The 1D advection equation

The advection equation at constant speed is the standard benchmark problem to test a code solving PDE equations. The exact analytical solution is known, allowing an investigation of the accuracy of the scheme. After a brief sketch of this equation, we develop a fully spectral method to solve the linear advection equation.

3.1. The general problem

The one dimensional advection equation with appropriate boundary and initial conditions, assuming a constant and positive speed $v > 0$ and a real parameter b , is given by

$$\frac{\partial u}{\partial t} + v \frac{\partial u}{\partial x} = b u + f \tag{18}$$

$$u(x, -1) = u_0(x) \tag{19}$$

$$u(-1, t) = B_G(t) \tag{20}$$

Note that compatibility between spatial and temporal boundary conditions requires $B_G(-1) = u_0(-1)$. We look for solutions $u(x, t)$ for spacetime coordinates $(x, t) \in [-1, 1]^2$, initial condition $u_0(x)$ and left boundary condition $B_G(t)$. The exact analytical solution is known. It corresponds to a propagation along the characteristic defined by $dt/ds = 1$ and $dx/ds = v$ and satisfies $du/ds = du/dt = bu$. Explicitly, the solution reads

$$u(x, t) = u_0(x - v(t - t_0)) e^{bt} + B_G\left(t - \frac{x - x_0}{v}\right) H(v(t - t_0) - (x - x_0)) \quad (21)$$

where H is the Heaviside unit step function and $x_0 = t_0 = -1$. Physically, the signal $u_0(x)$ travels along the positive x -axis at speed v (compatible with the left boundary condition $B_G(t)$) with an exponential decrease (resp. increase) in time according to e^{bt} for $b > 0$ (resp. $b < 0$).

3.2. Spectral method in space and time

Approximate solutions are found by expanding the unknown function $u(x, t)$ as a double Chebyshev series in both space and time. We seek solutions of the two variables $(x, t) \in [-1, 1]^2$ such that

$$u_N(x, t) = \sum_{i=0}^{N_x-1} \sum_{k=0}^{N_t-1} u_i^k T_i(x) T_k(t) \quad (22)$$

The number of expansion coefficients in space is labeled N_x whereas the one in time is labeled N_t . Obviously, they are not restricted to be equal.

The spatial and temporal first order derivatives of this expansion are obtained from the matrix operator $\mathcal{D}_{kl}^{(x)}$ and $\mathcal{D}_{kl}^{(t)}$, the superscripts x and t label the differentiation against spatial and temporal coordinates respectively. Note that these matrices are squared but their dimensions are not necessarily the same, resp. N_x and N_t . The time and space derivatives are given respectively by

$$\frac{\partial u_N}{\partial t}(x, t) = \sum_{i=0}^{N_x-1} \sum_{k=0}^{N_t-1} \sum_{l=0}^{N_t-1} \mathcal{D}_{kl}^{(t)} u_i^l T_i(x) T_k(t) \quad (23)$$

$$\frac{\partial u_N}{\partial x}(x, t) = \sum_{i=0}^{N_x-1} \sum_{k=0}^{N_t-1} \sum_{j=0}^{N_x-1} \mathcal{D}_{ij}^{(x)} u_j^k T_i(x) T_k(t) \quad (24)$$

From this, we deduce the full expression of the linear operator for the advection equation, being

$$\frac{\partial u_N}{\partial t}(x, t) + v \frac{\partial u_N}{\partial x}(x, t) - b u_N(x, t) \quad (25)$$

$$= \sum_{i=0}^{N_x-1} \sum_{k=0}^{N_t-1} \left[\sum_{l=0}^{N_t-1} \mathcal{D}_{kl}^{(t)} u_i^l + v \sum_{j=0}^{N_x-1} \mathcal{D}_{ij}^{(x)} u_j^k - b u_i^k \right] T_i(x) T_k(t) \quad (26)$$

$$= \sum_{i,j=0}^{N_x-1} \sum_{k,l=0}^{N_t-1} \left[\mathcal{D}_{kl}^{(t)} \delta_{ij} + v \mathcal{D}_{ij}^{(x)} \delta_{kl} - b \delta_{ij} \delta_{kl} \right] u_j^l T_i(x) T_k(t) \quad (27)$$

If present, we expand the source term similarly

$$f_N(x, t) = \sum_{i=0}^{N_x-1} \sum_{k=0}^{N_t-1} f_i^k T_i(x) T_k(t) \quad (28)$$

The unknowns u_i^k have to satisfy the advection equation in the interior of the integration domain. It is convenient to introduce the four dimensional matrix defined by

$$\mathcal{A}_{ijkl} = \mathcal{D}_{kl}^{(t)} \delta_{ij} + v \mathcal{D}_{ij}^{(x)} \delta_{kl} - b \delta_{ij} \delta_{kl} \quad (29)$$

such that the four dimensional system to solve reads

$$\sum_{j=0}^{N_x-1} \sum_{l=0}^{N_t-1} \mathcal{A}_{ijkl} u_j^l = f_i^k \quad (30)$$

The two indices i and k run from 0 to $N_x - 1$ and from 0 to $N_t - 1$ respectively. This does not yet include the boundary and initial conditions.

Indeed, in order to be able to impose adequate initial and boundary conditions, we use the penalty method, stating that

$$\frac{\partial u_N}{\partial t}(-1, t) + v \frac{\partial u_N}{\partial x}(-1, t) + \tau v (u_N(-1, t) - B_G(t)) = 0 \quad (31)$$

$$\frac{\partial u_N}{\partial t}(x, -1) + v \frac{\partial u_N}{\partial x}(x, -1) + \tau (u_N(x, -1) - u_0(x)) = 0 \quad (32)$$

τ is a parameter that must be large enough to ensure stability of the scheme. Typically we took $\tau = N(N + 1)/2$. Thus we have to add the appropriate

terms in the matrix \mathcal{A}_{ijkl} and right-hand-side f_i^k . Noting that

$$u(x, -1) = \sum_{i=0}^{N_x-1} \sum_{k=0}^{N_t-1} u_i^k T_i(x) T_k(-1) \quad (33)$$

$$= \sum_{i=0}^{N_x-1} \sum_{k=0}^{N_t-1} (-1)^k u_i^k T_i(x) \quad (34)$$

we need to include terms like $(-1)^k u_i^k$ into the matrix elements \mathcal{A}_{ijkl} . Similarly, for the initial profile, we get in terms of its expansion coefficients

$$u_0(x) = \sum_{i=0}^{N_x-1} u_{0i} T_i(x) \quad i \in [0..N_x - 1] \quad (35)$$

Thus, the quantities u_{0i} should be added to the right-hand-side element f_i^k . Following the same lines, the boundary condition is expressed as

$$u(-1, t) = \sum_{i=0}^{N_x-1} \sum_{k=0}^{N_t-1} u_i^k T_i(-1) T_k(t) \quad (36)$$

$$= \sum_{i=0}^{N_x-1} \sum_{k=0}^{N_t-1} (-1)^i u_i^k T_k(t) \quad (37)$$

Projecting the boundary function $B_G(t)$ on the polynomial basis gives

$$B_G(t) = \sum_{k=0}^{N_t-1} B_{Gk} T_k(t) \quad k \in [0..N_t - 1] \quad (38)$$

These terms $(-1)^i u_i^k$ and B_{Gk} must also be appropriately included in the matrices \mathcal{A}_{ijkl} and f_i^k . Note the similarity between initial Eq. (35) and boundary Eq. (38) conditions. Space and time are treated equally.

Finally, Eq. (30) is converted into a classical two dimensional linear algebra problem by a change of variables. For the unknown vector containing all the unknown quantities u_i^k , we write

$$z_s = u_j^l \quad (39)$$

with $s = j + l N_x$. The matrix is changed into

$$A_{rs} = \mathcal{A}_{ijkl} \quad (40)$$

with $r = i + k N_x$ and the right hand side into

$$h_r = f_i^k \quad (41)$$

Finally, the system is rewritten into

$$\sum_{s=0}^{N_x N_t - 1} A_{rs} z_s = h_r \quad (42)$$

with $r \in [0..N_x N_t - 1]$.

This completes the translation of the PDE into a linear system for the set of coefficients u_i^k . It is a well posed problem, invertible with standard linear algebra techniques.

4. The wave equation

4.1. Basics

Another important equation arising very often in physical systems is the wave equation. In Cartesian coordinates, supplemented with appropriate initial conditions, it reads

$$\frac{\partial^2 u}{\partial t^2}(x, t) - v^2 \frac{\partial^2 u}{\partial x^2}(x, t) = f(x, t) \quad (43)$$

$$u(x, -1) = u_0(x) \quad (44)$$

$$\frac{\partial u}{\partial t}(x, -1) = v_0(x) \quad (45)$$

Initial profile $u_0(x)$ and first time derivative $v_0(x)$ must be given. The boundary conditions can be outgoing waves on both sides

$$\frac{\partial u}{\partial t}(\pm 1, t) \pm v \frac{\partial u}{\partial x}(\pm 1, t) = 0 \quad (46)$$

or fixed boundaries, vanishing for instance on both sides

$$u(\pm 1, t) = 0 \quad (47)$$

or a mix between both types, outgoing on one side and fixed on the other side.

4.2. Spectral method in space and time

The method follows exactly the same lines as for the advection problem. The unknown function is expanded according to Eq.(22).

The full linear operator representing the wave equation becomes

$$\frac{\partial^2 u_N}{\partial t^2}(x, t) - v^2 \frac{\partial^2 u_N}{\partial x^2}(x, t) \quad (48)$$

$$= \sum_{i=0}^{N_x-1} \sum_{k=0}^{N_t-1} \left[\sum_{l=0}^{N_t-1} (\mathcal{D}_{kl}^{(t)})^2 u_i^l - v^2 \sum_{j=0}^{N_x-1} (\mathcal{D}_{ij}^{(x)})^2 u_j^k \right] T_i(x) T_k(t) \quad (49)$$

$$= \sum_{i,j=0}^{N_x-1} \sum_{k,l=0}^{N_t-1} \left[(\mathcal{D}_{kl}^{(t)})^2 \delta_{ij} - v^2 (\mathcal{D}_{ij}^{(x)})^2 \delta_{kl} \right] u_j^l T_i(x) T_k(t) \quad (50)$$

We expand the source term similarly

$$f_N(x, t) = \sum_{i=0}^{N_x-1} \sum_{k=0}^{N_t-1} f_i^k T_i(x) T_k(t) \quad (51)$$

The unknowns u_i^k have this time to satisfy the wave equation in the interior of the integration domain with special care for imposing the boundary and initial conditions. It is convenient to introduce another four dimensional matrix defined by

$$\mathcal{O}_{ijkl} = (\mathcal{D}_{kl}^{(t)})^2 \delta_{ij} - v^2 (\mathcal{D}_{ij}^{(x)})^2 \delta_{kl} \quad (52)$$

such that the four dimensional system to solve reads

$$\sum_{j=0}^{N_x-1} \sum_{l=0}^{N_t-1} \mathcal{O}_{ijkl} u_j^l = f_i^k \quad (53)$$

Here also, the two indices i and k run from 0 to $N_x - 1$ and from 0 to $N_t - 1$ respectively.

The matrix is completed by imposing initial conditions. For the unknown function, it reads

$$u_N(x, -1) = \sum_{i=0}^{N_x-1} \sum_{k=0}^{N_t-1} u_i^k T_i(x) T_k(-1) \quad (54)$$

$$= \sum_{i=0}^{N_x-1} \sum_{k=0}^{N_t-1} (-1)^k u_i^k T_i(x) \quad (55)$$

This leads to a linear system

$$u_0(x) = \sum_{i=0}^{N_x-1} u_{0i} T_i(x) \quad i \in [0..N_x - 1] \quad (56)$$

For its first time derivative, we have

$$\frac{\partial u_n}{\partial t}(x, -1) = \sum_{i=0}^{N_x-1} \sum_{k=0}^{N_t-1} u_i^k T_i(x) T_k'(-1) \quad (57)$$

$$= \sum_{i=0}^{N_x-1} \sum_{k=0}^{N_t-1} (-1)^{k+1} k^2 u_i^k T_i(x) \quad (58)$$

Next, using the boundary values for the Chebyshev first derivatives, we are led to another linear system

$$v_0(x) = \sum_{i=0}^{N_x-1} v_{0i} T_i(x) \quad i \in [0..N_x - 1] \quad (59)$$

Let us finish to describe the algorithm by implementing the boundary conditions. On one side, for outgoing wave conditions on both ends, at $x = +1$ and $x = -1$, they respectively translate into

$$\sum_{j=0}^{N_x-1} \sum_{l=0}^{N_t-1} \left[\mathcal{D}_{kl}^{(t)} + v j^2 \delta_{kl} \right] u_j^l = 0 \quad (60)$$

$$\sum_{j=0}^{N_x-1} \sum_{l=0}^{N_t-1} (-1)^j \left[\mathcal{D}_{kl}^{(t)} + v j^2 \delta_{kl} \right] u_j^l = 0 \quad (61)$$

for $k \in [0..N_t - 1]$. On the other side, for fixed and vanishing boundary conditions on both ends, it reduces to

$$\sum_{j=0}^{N_x-1} u_j^l = 0 \quad (62)$$

$$\sum_{j=0}^{N_x-1} (-1)^j u_j^l = 0 \quad (63)$$

for $l \in [0..N_t - 1]$. This gives another set of $2N_t$ equations for the matrix \mathcal{O} .

Eq. (53) is converted into another classical two dimensional linear algebra problem by the same change of variables except that the matrix is now

$$O_{rs} = \mathcal{O}_{ijkl} \quad (64)$$

and the new system

$$O_{rs} z_s = h_r \quad (65)$$

z_s and h_r being already defined for the advection problem. The same definition applies here except for the indices limits.

5. The 2D diffusion equation

Solving the diffusion equation requires usually a very small explicit finite difference time stepping, preventing from a large time span simulation. Therefore, this part of a PDE is solved by some implicit time schemes, like the second order Crank-Nicholson algorithm. Infinite spectral order of accuracy can be recovered by performing a spectral expansion in time as shown in this paragraph. Moreover, it applies to any number of spatial dimensions, we demonstrate the feasibility for two-dimensional space configurations.

Let us consider the diffusion equation in the domain $(x, y) \in [-1, 1]^2$ for $t \in [-1, 1]$ such that

$$\frac{\partial u}{\partial t}(x, y, t) = \eta(x, y, t) \left[\frac{\partial^2 u}{\partial x^2}(x, y, t) + \frac{\partial^2 u}{\partial y^2}(x, y, t) \right] \quad (66)$$

$$u(x, y, -1) = u_0(x, y) \quad (67)$$

The initial profile $u_0(x, y)$ must be specified and η is the diffusion coefficient. We enforce Dirichlet boundary conditions on the border of the domain such that

$$u(\pm 1, \pm 1, t) = 0 \quad (68)$$

Imposing other boundary conditions, like Neumann or Robin type is straightforward. We use the Chebyshev collocation method to solve the homogeneous boundary conditions by introducing the basis of Chebyshev polynomials $T_k(x)$. Our choice is guided by a possible extension of this algorithm to non-linear problems; it is easier to work in physical space compared to the coefficient space, especially for products of the non-linear terms and non constant diffusion coefficient or other spatially varying characteristics of the problem under investigation.

The homogeneous boundary conditions are imposed by a Chebyshev collocation method to get the linear system satisfied by the coefficients of the interpolant u_N given by an expansion like

$$u_N(x, y, t) = \sum_{i=0}^{N_x} \sum_{j=0}^{N_y} \sum_{k=0}^{N_t} u_{ijk} T_i(x) T_j(y) T_k(t) \quad (69)$$

The spatial and temporal derivatives of the interpolant u_N are immediately obtained from those of $\phi_i(x)$.

For the points of discretisation, we get a linear system for the unknown coefficients u_{ijk} as

$$L u = g \quad (70)$$

where the square matrix L is obtained following the indexing method proposed by [2] as

$$L_{rs} = T_i(x_l) T_j(y_m) T'_k(t_n) - \eta(x_l, y_m, t_n) [T''_i(x_l) T_j(y_m) T_k(t_n) + T_i(x_l) T''_j(y_m) T_k(t_n)] \quad (71)$$

We do not give explicit expressions for the indices (r, s) , the collapsing of (i, j, l) being clearly exposed in [2] for 2D problems. Extension to our 3D problem is straightforward. Note also that the right-hand-side vector g in Eq. (70) contains the initial $u_0(x_l, y_m)$ as well as the boundary conditions.

Now we have all the tools necessary to check and test the code, especially the treatment of the boundary conditions. We discuss the results in the next sections.

6. Check and test of the algorithm

We now give some typical applications to check our algorithm on simple initial value problems like advection and wave propagation. Different boundary conditions are also investigated for the wave equation.

6.1. Advection equation

Our advection equation at constant positive speed propagates a signal along the positive x -axis. For the initial value, we take either a Gaussian shape vanishing at the boundaries $x = \pm 1$ (in order to remain consistent with the boundary conditions) like

$$u_0(x) = (1 - x^2) e^{-10x^2} \quad (72)$$

or simply zero $u_0(x) = 0$ but with incoming signal from the left or a source term. Actually we tried this prescription and could not get errors less than 10^{-7} (see definition of the error below) because the prescribed initial profile is not infinitely smooth at the boundary ± 1 . We therefore tried a more smooth function at these boundaries such that they are satisfied within numerical accuracy. The basic idea is to use a bunch of shifted Gaussians such that

$$u_0(x) = e^{-10x^2} - e^{-10(x-2)^2} - e^{-10(x+2)^2} + e^{-10(x-4)^2} + e^{-10(x+4)^2} \quad (73)$$

This way, u_0 remains very close to zero and behaves smoothly, see for instance [3].

We performed different sets of run. In the first set, the choice of a Gaussian is useful to look for outgoing waves, fixing the left boundary to zero. In a second set, the vanishing initial condition is set up in order to test in-going left boundary conditions. For instance we took a incoming signal such that for $x = -1$

$$B_G(t) = \sin(2\pi t) \quad (74)$$

This is applied on the left side at any time $t \in [-1, 1]$. The particular choice of a frequency of $\omega = 2\pi$ ensures to get exactly one period inside the simulation box at the final time of simulation. Any other value would also be fine.

Finally, in a last set of runs, a source term has been add, prescribed as a harmonic function in time and Gaussian shape in space as follows

$$s(x, t) = \frac{\sin(2\pi t)}{2\pi} (1 - x^2) e^{-20x^2} \quad (75)$$

In order to avoid pollution of the solution by inhomogeneous boundary conditions, in this case, we force again the left boundary to zero.

Let us have a look on some results for each set of runs. The Gaussian signal travelling along the positive x -axis is depicted in a space-time plot in Fig. 1 with a constant speed $v = 1$. There is no incoming information from the left side $x = -1$, it is imposed to zero therefore remaining at these value during the full time span. As expected for these normalization constants, the characteristic curves are inclined to 45° with respect to the time axis. The signal leaves the simulation box on the right side $x = 1$ without any spurious oscillation or other undesirable effects. The numerical implementation of the outgoing wave condition is perfectly reproduced by our algorithm, to machine accuracy.

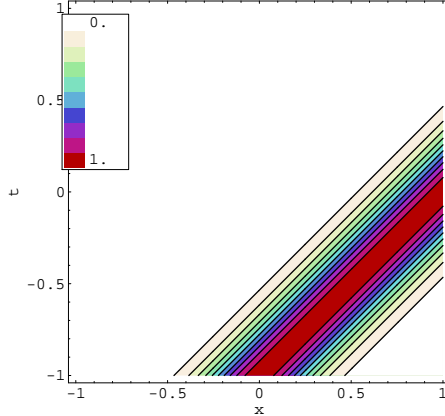


Figure 1: Solution of the advection equation for the initial Gaussian function and no incoming information, $B_G(t) = 0$. The speed is set to unity, $v = 1$. No spurious effects appear on the boundaries.

N_x	N_t	error
5	5	1.221E-01
9	9	1.044E-01
17	17	1.661E-02
33	33	6.218E-06
65	65	1.668E-10
129	129	4.799E-11

Table 1: Convergence properties for the advection equation. The error is plotted against the number of discretisation points, being the same in x and t coordinates.

Moreover, the convergence properties are checked by inspecting the behavior of the error against the number of collocation points. We define this error by

$$\epsilon = \max_{(i,k) \in [0..N-1]^2} |u_{\text{an}}(x_i, t_k) - u_{\text{num}}(x_i, t_k)| \quad (76)$$

where u_{an} corresponds to the exact analytical solution Eq. (21) and u_{num} to the numerical spectral approximation.

The trend is summarized in tab. 1. The minimum relative error falls down to less than 10^{-10} . This is achieved for a number of discretisation points $N_x = N_t = 129$, the maximum we can reach on our computer.

Next we consider the second set of runs where homogeneous initial con-

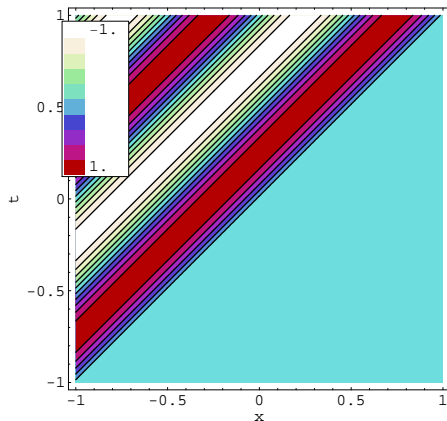


Figure 2: Solution of the advection equation with incoming left boundary condition. The imposed sinusoidal wave propagates to the right with speed $v = 1$. No spurious effects appear on the boundaries.

ditions $u_0(x) = 0$ are employed supplemented with left boundary incoming signal prescribed by Eq. (74). The corresponding space-time plot is shown in Fig. 2. As expected, the imposed sinusoidal wave propagates to the right with constant speed $v = 1$. No spurious effects appear on any boundary. At the final time of the simulation, the solution matches the function $\sin(2\pi x)$ containing one period of the trigonometric sin function as would be expected from the exact analytical solution.

Finally, for the last set of runs, we still start with homogeneous initial conditions $u_0(x) = 0$ and no left boundary incoming signal, but we add a source term f on the right hand side of the advection equation with Gaussian shape. Results are presented in Fig. 3. Perturbations from the source arise mostly in the middle of the box and are transported to the right along the positive x -axis and leave the computational domain very smoothly in accordance with the analytical expected solution.

This concludes the advection part. In this section, we demonstrated that a fully spectral method in both space and time can be used to solve partial differential equations like the advection problem. No particular problem arises to treat properly the boundary conditions or the source term. Outgoing waves are handled to machine accuracy.

In the following paragraph, we show that the same conclusions apply well to the wave equation.

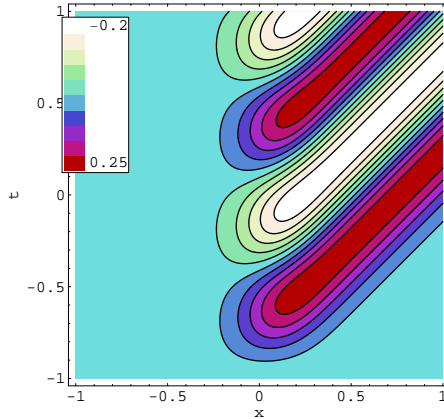


Figure 3: Solution of the advection equation with a source term. Here also, no spurious effects appear on the boundaries.

6.2. Wave equation

For the wave equation, we use the same initial conditions as those previously explained. However, supplementary initial and boundary value conditions must be imposed because it is second order in both space and time. Thus, the first order time derivative must be given. We took simply

$$\frac{\partial}{\partial t}u_0(x) = 0 \quad (77)$$

with additional boundary conditions on the left and right ends.

Fixed left and right boundary conditions are also interesting in order to check the perfect reflection of the wave on both sides of the computational domain. We discuss the results in detail now.

In Fig. 4 the space-time plot of the solution to the outgoing wave problem is presented for the initial Gaussian shape. As expected, it splits into two equal parts, one propagating to the left at speed $v = 1$ and the other to the right at the same speed. When reaching the boundaries, they leave the integration domain, and the box remains empty with $u(x, t) = 0$ after a while. Boundary conditions are correctly implemented, no oscillations or divergence are reported.

Next we consider an incoming wave from the right side, with sinusoidal temporal variations, the same as for advection and outgoing left boundary.

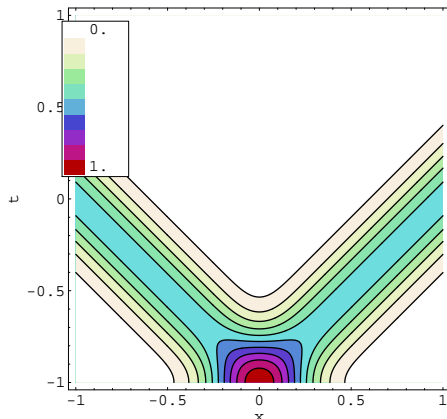


Figure 4: Solution of the wave equation with outgoing wave conditions and an initial Gaussian profile. Two waves emerge propagating in opposite direction with speed $v = 1$. They leave the simulation box perfectly, no spurious effects.

This sinusoidal shape fills the entire box at the end of simulation. Fig. 5 summarizes the trend, the characteristic curves are inclined to 45° in accordance with $v = 1$. Instead of an incoming wave, we replace it next by a source inside the box, like a radiating system. The solution is given in Fig. 6. The same remarks as before apply, outgoing waves are correctly implemented and well reproduced.

Finally, we look for reflecting boundary conditions on either one or two sides. Consider again the initial condition of Fig. 4 but with fixed vanishing boundaries. In such a case, the wave is perfectly reflected and travels back in opposite direction. This is clearly seen in Fig. 7. Note however that this time we took $v = 2$ in order to simulate a full back and forth reflection with the final state equal to the initial state, allowing easy comparison and investigation of the accuracy. We know that at the end, we should retrieve the initial Gaussian shape $u_0(x)$. This is indeed the case. In addition, the evolution of the relative error between initial and final state is shown in Tab. 2. It saturates at a level around 10^{-10} for $N_x = N_t = 129$.

Last, we use again vanishing initial conditions with right incoming sinusoidal wave but left reflecting boundary instead of outgoing wave. In this case, ingoing and outgoing waves overlap to form a stationary pattern with crests and nodes as seen in Fig 8, it is equal to $\sin(\pi x)$. It is instructive to compare this plot with Fig 5. Their solutions are equal until the signal

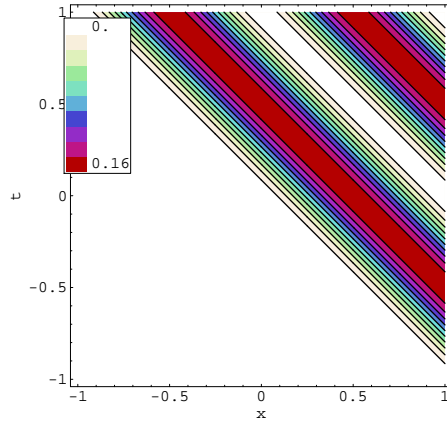


Figure 5: Solution of the wave equation with initial homogeneous and vanishing conditions but right incoming sinusoidal wave.

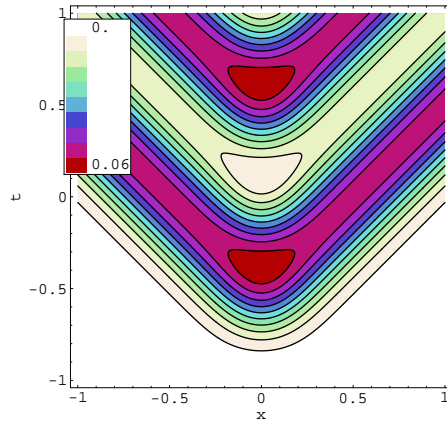


Figure 6: Solution of the wave equation with initial homogeneous and vanishing conditions. A source term is added and outgoing wave boundaries are imposed.

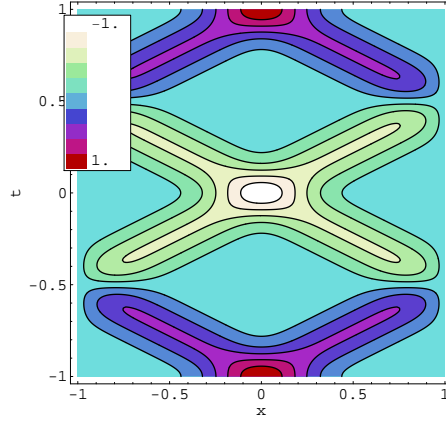


Figure 7: Solution of the wave equation for reflecting boundary conditions starting with an initial Gaussian shape.

N_x	N_t	error
5	5	6.093E-01
9	9	1.116E+00
17	17	2.170E-01
33	33	2.416E-02
65	65	8.525E-07
129	129	9.858E-11

Table 2: Convergence properties for the wave equation for reflecting boundary conditions, fig 7. The error is plotted against the number of discretisation points, being the same in x and t .

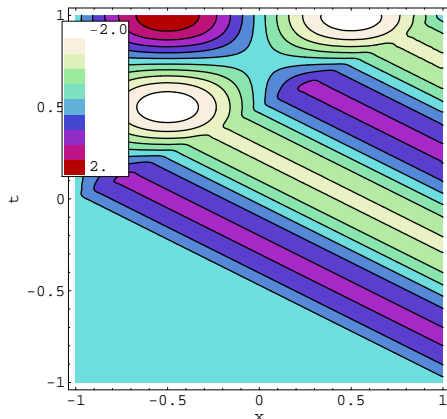


Figure 8: Solution of the wave equation with fixed left boundary condition and incoming wave from the right. After a while, at the end of the run, a stationary wave settles down with crests and nodes.

reaches the left wall where reflection starts (within a factor two in timescale because the speeds are different $v = 1$ against $v = 2$).

6.3. 2D diffusion equation

We close the tests by looking for a two space dimension problem symbolize by a diffusion process as described before. For the sake of simplicity, we only look for uniform diffusion coefficient within the computational domain, namely $\eta(x, y, t) = \text{cste}$, the reason being that analytical solutions are easily derived. Obviously, the algorithm can handle non uniform diffusion coefficients without any modification.

The initial profile is given by a double sinusoidal profile such that

$$u_0(x, y) = \sin(\pi x) \sin(\pi y) \quad (78)$$

The exact solution is then given by

$$u_{\text{an}}(x, y, t) = \sin(\pi x) \sin(\pi y) e^{-2\eta\pi^2 t} \quad (79)$$

The error is shown in Tab. 3. Due to memory overflow, we could not perform resolutions better than $33 \times 33 \times 33$. Nevertheless, already with a moderate $17 \times 17 \times 17$ resolution, we got an error of only 10^{-13} . As expected, the exponential decrease of the error with increasing number of collocation points is recovered, spectral accuracy is achieved. Including a spatially varying diffusion coefficient is straightforward.

N_x, N_y	N_t	error
5	5	6.602E-03
9	9	4.194E-06
17	17	1.065E-13
33	33	5.300E-13

Table 3: Convergence properties for the diffusion equation. The error is plotted against the number of discretisation points, being the same in x and t .

7. Conclusion

In this paper, we demonstrated the ease to implement a numerical algorithm with fully spectral methods in both space and time. We applied it to three important classes of problems which are the advection, diffusion and wave equations. The great advantage of our method is that the treatment is symmetric with respect to space and time variable. This reflects in the imposition of the boundary conditions. We showed examples for the linear advection, diffusion and wave equations and recover spectral accuracy as expected. Different methods were also employed, like penalty, tau and Galerkin collocation.

The main drawback of the method is the necessity to invert a large sparse matrix. This limits drastically the number of discretisation points as well as the number of spatial dimensions. For multi space dimensional purposes, the required memory quickly overwhelms the available capacities of any computer. Moreover the time spend to invert the matrix becomes prohibitive. In future work, it is desirable to adapt the algorithm and put some effort to come over this difficulty by employing iterative methods for solving the corresponding large algebraic linear system.

Extension to cylindrical and spherical geometry are also planed, as those coordinate systems are better adapted to our astrophysical interests, for instance accretion disks or structure of stars. Thanks to the multiplication matrices \mathcal{P} introduced in this paper, the discretised version of any linear differential operator is derived easily. However, outgoing wave boundary conditions in arbitrary geometry need a more careful treatment. This is left for future work.

The preliminary study presented in this paper was aimed to demonstrate that fully spectral method are easy to design even for two space dimensions. We hope that it will serve as a starting point to those willing to use such

techniques for their own particular applications.

References

- [1] Birdsall, C. & Langdon, A. 2005, Plasma physics via computer simulation (IOP Publishing)
- [2] Boyd, J. P. 2001, Chebyshev and Fourier Spectral Methods (Springer-Verlag)
- [3] Boyle, M., Lindblom, L., Pfeiffer, H. P., Scheel, M. A., & Kidder, L. E. 2007, Phys. Rev. D, 75, 024006
- [4] Canuto, C., Hussaini, M., Quarteroni, A., & Zang, T. 2006, Spectral Methods. Fundamentals in Single Domains (Springer-Verlag)
- [5] Canuto, C., Hussaini, M., Quarteroni, A., & Zang, T. 2007, Spectral Methods. Evolution to Complex Geometries and Applications to Fluid Dynamics (Springer Verlag)
- [6] Don, W., Gottlieb, D., & Jung, J. 2003, Journal of Computational Physics, 192, 325
- [7] Grandclément, P. & Novak, J. 2009, Living Reviews in Relativity, 12
- [8] Hennig, J. & Ansorg, M. 2009, Journal of Hyperbolic Differential Equations, 6, 161
- [9] Hockney, R. W. & Eastwood, J. W. 1988, Computer simulation using particles, ed. Hockney, R. W. & Eastwood, J. W.
- [10] Ierley, G., Spencer, B., & Worthing, R. 1992, Journal of Computational Physics, 102, 88
- [11] Press, W. H., Teukolsky, S. A., Vetterling, W. T., & Flannery, B. P. 1992, Numerical recipes in C. The art of scientific computing (Cambridge: University Press, —c1992, 2nd ed.)